Published in final edited form as:
*Vision Res*. 2008 February ; 48(3): 413–423.

# Spatial Distribution of Intraflagellar Transport Proteins in Vertebrate Photoreceptors

**Katharine Luby-Phelps**[1,3], **Joseph Fogerty**[1], **Sheila A. Baker**[1,4], **Gregory J. Pazour**[2], and **Joseph C. Besharse**[1]

1*Dept. Cell Biology, Neurobiology & Anatomy, Medical College of Wisconsin, Milwaukee, WI.*

2*Program in Molecular Medicine, University of Massachusetts Medical School, Worcester, MA.*

## Abstract

Intraflagellar transport (IFT) of a ~17S particle containing at least 16 distinct polypeptides is required for the assembly and maintenance of cilia and flagella. Although both genetic and biochemical evidence suggest a role for IFT in vertebrate photoreceptors, the spatial distribution of IFT proteins within photoreceptors remains poorly defined. We have evaluated the distribution of 4 IFT proteins using a combination of immunocytochemistry and rod-specific over-expression of GFP tagged IFT proteins. Endogenous IFT proteins are most highly concentrated within the inner segment, around the basal body, and within the outer segment IFT proteins are localized in discrete particles along the entire length of the axoneme. IFT52-GFP and IFT57-GFP mimicked this pattern in transgenic *Xenopus*.

### Keywords

Photoreceptor; connecting cilium; microtubule; intraflagellar transport; kinesin

## INTRODUCTION

Vertebrate photoreceptors are composed of an inner segment responsible for macromolecular synthesis and an outer segment involved in phototransduction. The two segments are bridged by the connecting cilium, which contains a 9 + 0 axoneme that projects through the connecting cilium and into the outer segment (Besharse & Horst, 1990). The outer segment forms developmentally by modification of the membrane of the sensory cilium to form the discs of the outer segment. Initial development of the outer segment requires prodigious macromolecular transport through the connecting cilium to form these discs. The requirement for transport continues throughout the life of the cell as ~ 10% of the distal ends of the outer segments are shed each day and phagocytosed by the surrounding retinal pigmented epithelium. Replacement material is synthesized in the inner segment and transported to the outer segment through the connecting cilium (Young, 1967). In addition to anterograde transport of

**Correspondence:** Dr. Joseph C. Besharse Marvin Wagner Professor and Chair Department of Cell Biology, Neurobiology and Anatomy Medical College of Wisconsin 8701 Watertown Plank Road Milwaukee, WI 53226−0509 Phone: 414−456−8261 Fax: 414−456−6517 E-mail: jbeshars@mcw.edu.
[3]Present address: Dept. of Cell Biology, University of Texas Southwestern Medical Center, 5323 Harry Hines Blvd., Room K2.220, Dallas, TX 75390−9039.
[4]Present address: Dept. Ophthalmology, Duke University Medical Center, Erwin Road, Durham, NC 27707.

components required for maintenance of the outer segment, proteins involved in phototransduction such as arrestin and transducin shuttle between the inner and outer segments in a light-dependent manner (Mendez, Lem, Simon & Chen, 2003, Peterson, Tam, Moritz, Shelamer, Dugger, McDowell, Hargrave, Papermaster & Smith, 2003, Sokolov, Lyubarsky, Strissel, Savchenko, Govardovskii, Pugh & Arshavsky, 2002). While the mechanism of transport between the inner and outer segments is not known in detail, intraflagellar transport (IFT), which is required for the assembly and maintenance of cilia and flagella in a variety of systems, is likely to play a significant role.

IFT was first described in the motile flagella of *Chlamydomonas* (Kozminski, Johnson, Forscher & Rosenbaum, 1993) and has since been observed in a variety of motile and non-motile cilia (for reviews, see (Pazour, Baker, Deane, Cole, Dickert, Rosenbaum, Witman & Besharse, 2002, Scholey, 2003, Sloboda, 2005)). IFT involves the transport of a large complex of at least 16 polypeptides along the outer doublet microtubules of the axoneme, beneath the plasma membrane, at rates ranging from 0.7 to 2 μm/sec for anterograde transport and 1 to 3.5 μm/sec for retrograde transport (Rosenbaum & Witman, 2002). Genetic evidence indicates that both heterotrimeric and homodimeric members of the kinesin 2 family serve as anterograde transport motors (Cole, Diener, Himelblau, Beech, Fuster & Rosenbaum, 1998, Kozminski, Beech & Rosenbaum, 1995, Snow, Ou, Gunnarson, Walker, Zhou, Brust-Mascher & Scholey, 2004), while a cytoplasmic dynein based on Dhc1b/2 heavy chain is the motor for transport in the retrograde direction (Pazour, Wilkerson & Witman, 1998, Signor, Wedaman, Orozco, Dwyer, Bargmann, Rose & Scholey, 1999) (Pazour, Dickert & Witman, 1999).

Involvement of IFT in photoreceptors is strongly supported by the immunolocalization of kinesin II and endogenous IFT proteins to the basal body and connecting cilium (Beech, Pagh-Roehl, Noda, Hirokawa, Burnside & Rosenbaum, 1996, Pazour et al., 2002), and the finding that bovine photoreceptors contain a ~17S IFT protein complex similar to that of motile flagella (Baker, Freeman, Luby-Phelps, Pazour & Besharse, 2003). Furthermore, mice with a deletion of the kinesin II subunit, Kif3A, or a hypomorphic mutation in the IFT complex protein, IFT88/polaris, exhibit failed outer segment morphogenesis, and miss-localization of opsin, which leads to loss of photoreceptors (Jimeno, Feiner, Lillo, Teofilo, Goldstein, Pierce & Williams, 2006, Marszalek, Liu, Roberts, Chui, Marth, Williams & Goldstein, 2000, Pazour et al., 2002).

Localization studies of IFT proteins in photoreceptors are limited to immunofluorescent images from frozen sections of mature bovine, mouse, or embryonic zebrafish retina (Pazour et al., 2002, Tsujikawa & Malicki, 2004), and provide only limited insight into the spatial distribution of IFT proteins within either the inner or outer segment. In the present study we have used mouse retinas along with the large photoreceptors of *Xenopus*, which contain axonemes that are substantially longer than those in mammals, to study the spatial distribution of IFT proteins in rods. Our data indicate that endogenous IFT proteins are most abundant in the inner segment and basal body region, and that within the outer segment IFT proteins are found in discrete particles along the entire length of the axoneme. Our data provide a higher resolution view of IFT protein distribution and indicate that IFT operates along the entire length the outer segment rather than just within the connecting cilium.

## METHODS

### IFT Constructs

RNA was extracted from *Xenopus* retina using Trizol (Invitrogen, ,Carlsbad, CA, USA). Reverse transcription was carried out using AMV-RT (Promega, Madison, WI, USA) with an oligo-dT primer, followed by PCR with two degenerate primers based on the sequences for known homologs of IFT20: 5'-CTGGACCCCGAGGTGACNCARCARAC-3' and 5'-

CGCCGATGGCCTTCATYTTYTCRTT-3'. The product was cloned into pCRII-TOPO (Invitrogen,, Carlsbad, CA, USA) and the full insert was sequenced. The clone was not full length, but matched a *Xenopus* EST from Research Genetics (PBX0153F10), which contained the full-length cDNA (accession number AY048114). For transgenesis, the full-length sequence obtained by PCR from the Research Genetics EST was subcloned into pEGFP-1 (BD Biosciences Clontech, Palo Alto, CA, USA) downstream of a 5.5 kb fragment of the *Xenopus* rod opsin promoter (Kennedy, Vihtelic, Checkley, Vaughan & Hyde, 2001, Knox, Schlueter, Sanger, Green & Besharse, 1998). For transfection of tissue culture cells, the sequence was subcloned into pcDNA3.1/CT-GFP (Invitrogen,, Carlsbad, CA, USA) . The full coding sequence from mouse cDNAs for mouse IFT88, 57 and 52 (Pazour et al., 2002) were subcloned into the same vectors as IFT20. LLC-PK1 cells (American Type Culture Collection, Manassas, VA, USA) were transfected with CMV-IFT20-GFP or IFT88-GFP using Lipofectamine 2000 (Invitrogen , Carlsbad, CA, USA) according to the manufacturer's instructions.

## Transgenic Animals

*Xenopus* transgenesis was carried out using a restriction enzyme mediated method as described previously (Knox et al., 1998). Transgenic embryos were screened at stage 43 for GFP expression in the eye. Positive animals were euthanized at stage 45 or later, and the eyes were enucleated. Eyes were dissected to expose the retina and mounted in a balanced salt solution (Cahill & Besharse, 1991) between two glass coverslips for fluorescence microscopy. Transgenesis was confirmed by genomic PCR as follows. Tails clipped from euthanized animals were digested in 0.4 mg/ml proteinase K overnight at 55 °C. DNA was extracted with 24:24:1 phenol:chloroform:isoamyl alcohol, precipitated with isopropanol and resuspended in an appropriate volume of TE buffer. The inserted gene was detected using primers for EGFP (5'-CAA GCT GAC CCT GAA GTT CAT CTG-3' and 5'-CGG ATC TTG AAG TTC ACC TTG ATG-3'). Animal care was in accordance with the US Public Health Service Policy on Humane Care and Use of Laboratory Animals.

## Antibodies

Antibodies against the mouse IFT88, 57, 52 and and 20 proteins were generated in rabbits and affinity purified as described previously (Pazour et al., 2002). A mouse monoclonal antibody directed against acetylated alpha-tubulin was purchased from Sigma (St. Louis, MO, USA, T6793?). Goat anti-rabbit and goat-anti-mouse antibodies coupled to Alexa 488 or Cy3 were purchased from Molecular Probes (Eugene, OR, USA) or Jackson ImmunoResearch Laboratories (West Grove, PA, USA). Goat anti-rabbit IgG coupled to horse radish peroxidase (HRP) was purchased from Amersham Biosciences (Piscataway, NJ, USA, Cat No. NA934).

## Western blotting

Retinas from adult *Xenopus laevis* were homogenized on ice in 10 mM HEPES, pH 7.2 containing a protease inhibitor cocktail (Sigma, St. Louis, MO, USA, Cat. #P--3840). Nonidet P-40 was added to a final concentration of 0.05%, the samples were incubated for 15 min on ice, and clarified at 25 psi in a Beckman airfuge (Beckman Coulter, Fullerton, CA, USA) for 10 min. Samples were boiled in Laemmli buffer and run on an 8% SDS polyacrylamide gel. Proteins were transferred to PVDF membrane and probed with rabbit antibodies against IFT proteins at a dilution of 1:1000. Goat anti-rabbit IgG coupled to HRP at a dilution of 1:5000 was used for chemiluminescent detection of polypeptides that cross-reacted with anti-IFT antibodies.

### Immunocytochemistry and Fluorescence Microscopy

Immunofluorescence localization was carried out on dissociated *Xenopus* rod outer segments (ROS) as described previously (Sale, Besharse & Piperno, 1988). The primary antibody was diluted 1:100 (IFT) or 1:200 (tubulin). Fluorescent secondary antibodies were diluted 1:200. To view GFP fluorescence in frozen sections, transgenic embryos were embedded in OCT/sucrose, frozen by immersion in liquid nitrogen, and 10 μm sagittal sections were cut through the eyes. Fluorescence was viewed by wide-field epifluorescence microscopy on a Nikon Eclipse TE300 inverted microscope (Nikon Instruments, Inc., Melville, NY, USA). Digital images were taken using a CoolSnap color camera (Roper Scientific, Tucson, AZ, USA) and saved as 48-bit raw TIFF images on a Macintosh G4 computer (Apple Computer, Cupertino, CA, USA). Confocal images were acquired on a TCS SP2 confocal microscope (Leica Microsystems, Bannockburn, IL, USA) using 40×, 1.25 NA or 60×, 1.32 NA oil immersion objectives, with the pinhole adjusted to one Airy disk unit. GFP fluorescence was excited with the 488 nm line of an argon laser. Adobe Photoshop (Adobe Systems, Inc., San Jose, CA, USA) was used to prepare images for publication. For image analysis regions of interest were defined interactively and the mean fluorescence intensity was measured using NIH Image 1.63. Mean background intensity was measured within each image and subtracted from the mean intensity of each region of interest. Intensity ratios, mean intensity ratios and standard errors were calculated using a Microsoft Excel worksheet.

### Electron Microscopy

The heads of *Xenopus* embryos that were positive for transgenesis by genomic PCR were fixed for 90 minutes on ice in 1% osmium tetroxide/1% glutaraldehyde in 0.067 M cacodylate buffer, pH 7.4 and prepared for thin-section electron microscopy by standard methods. Post-embedment immunolocalization at the EM level using 10 nm colloidal gold on LR-White sections was carried out as described previously (Pazour et al., 2002).

## RESULTS

### Immunogold Localization of IFT88 in Mouse Rods

Data on the spatial distribution of IFT proteins is currently limited to immunofluorescence images in mouse and bovine retina in which IFT proteins were most abundant around the region of the basal body, and with lesser labeling of the connecting cilium (Pazour et al., 2002). To further study IFT proteins in the vicinity of the basal body in the inner segment, we have carried out immunogold localization. To date this analysis is restricted to the use of IFT88 antibodies on LR-White sections from 21 day old mouse retina; a control in this anlysis is the 21 day old $Tg737^{orpk}$ mouse retina in which IFT88 protein is strongly reduced. As expected from the immunofluorescence analysis (Pazour et al., 2002), IFT88 was most abundant in the region immediately adjacent to the basal body and accessory centriole (see Figure 1A-D). Although at lower labeling density, IFT88 was also routinely detected in the connecting cilium (Figure 1E-G), and in the axoneme region adjacent to OS discs (Figure 1J-K). The distribution of IFT88 around the basal body and accessory centriole is consistent with the idea based on immunogold localization of IFT52 in *Chlamydomonas*, that transition fibers in this region are the docking sites for IFT particle assembly (Deane, Cole, Seeley, Diener & Rosenbaum, 2001). An important feature of our analysis was that the non-specific background staining was extremely low and that IFT88 appeared to be concentrated in discrete, electron opaque structures that labeled with multiple gold particles (Figure 1C, H, L, O). The details of these structures were often obscured by the gold particles and lacked contrast in LR-White sections. However, they are consistent with the idea that IFT88 is associated with IFT particles and/or vesicle-like structures in the region surrounding the basal body and accessory centriole. The high abundance of IFT88 in the vicinity of the basal body in wild type mice was in distinct contrast to the condition in 21 day old $Tg737^{orpk}$ mice (Figure 1P) where gold particles were extremely

difficult to find. The paucity of IFT88 in these cells is consistent with our earlier finding that the greatly reduced expression of IFT88 protein in Tg737$^{orpk}$ mice is associated with photoreceptor degeneration (Pazour et al., 2002).

### Expression and localization of endogenous IFT proteins in *Xenopus* rods

To further examine the spatial distribution of IFT proteins, particularly within the outer segment, we took advantage of the large rod photoreceptors of *Xenopus laevis*. To examine the expression of endogenous IFT proteins, extracts of retinas from adult *Xenopus laevis* were Western blotted using affinity purified rabbit antibodies to mouse IFT sequences. Antibodies to IFT 88, 57 and 52 specifically recognized polypeptides with apparent molecular weights of ~95, 57 and 50 kDa respectively (Figure 2). Antibodies to mouse IFT20 did not recognize any proteins in the *Xenopus* retinal extracts, but labeled photoreceptor outer segments in a manner similar to the other IFT antibodies (see below). Immunofluorescence on whole mounted outer segments showed that all four IFT proteins were abundant in the inner segment and were localized along the full length of the axoneme in a discrete, particulate pattern (Figure 3A-D). In all cases rod axonemes extended in excess of half the length of the outer segment as previously reported (Kaplan, Iwata & Sears, 1987,Sale et al., 1988), but in some cases they extended nearly the entire length of the OS (Figure 3A, B). In both whole mounted outer segments and confocal Z-series analysis of frozen sections, IFT proteins were highly concentrated near the basal body. Figure 3E and F illustrates two representative double-labeled Z-series for IFT57 (Figure 3E) and IFT20 (Figure 3F). Each series begins near the basal body (large arrows) and extends through an obliquely sectioned outer segment along the axoneme (red) showing discrete particles labeled with the anti-IFT antibody. A particulate organization of IFT staining is also apparent in the inner segment in the vicinity of the basal body. Here both IFT57 (Figure 3E, Slices 1−5) and IFT20 (Figure 3F, Slices 1−5) label particles below the level of the basal body.

### Rod-specific overexpression of IFT Proteins in *Xenopus* embryos

As an alternative to immunocytochemistry for analysis of spatial distribution, IFT proteins fused with enhanced GFP were targeted to the rods of transgenic *Xenopus* embryos using the *Xenopus* rod opsin promoter (Knox et al., 1998). Observations of IFT-GFP over-expression were best made by merging the GFP and the transmitted light image (Figure 4). For example, IFT52-GFP was found concentrated at the basal body in the inner segment and localized to the axoneme in the outer segment (Figure 4B-D); occasionally punctate particles were associated with the axoneme (arrowheads in Figure 4D). Similar observations were made for both IFT52-GFP (Figure 4 and Figure 5A-B) and IFT57-GFP (Figure 5C-D) in which GFP fusion proteins mimicked the pattern seen by immunocytochemistry in the outer segment. In addition, diffuse fluorescence was observed throughout the cytoplasm of the inner segment. Rods in the retinas of control animals over-expressing enhanced GFP alone sometimes also exhibited spatial variations in intensity in these regions (Figure 5E). Since GFP does not bind to intracellular components (Swaminathan, Hoang & Verkman, 1997, Terry, Matthews & Haseloff, 1995, Yokoe & Meyer, 1996), these variations in intensity reflect variable pathlength and/or accessible volume (Taylor & Wang, 1980) as was recently demonstrated for *Xenopus* rods (Peet, Bragin, Calvert, Nikonov, Mani, Zhao, Besharse, Pierce, Knox & Pugh, 2004, Taylor & Wang, 1980). Optical sections obtained by confocal microscopy with high NA objectives are of a uniform thickness that is well within the thickness of the cells, leaving accessible volume differences as the primary determinant of intensity variations in rods expressing enhanced GFP alone. Accessible volume in the region of the basal body is highly variable due to the large number of mitochondria clustered there. In the outer segment, accessible volume is highly restricted by the dense packing of the disks.

To rule out the possibility that the apparent localization of IFT52-GFP and IFT57-GFP to the basal body and axoneme was an artifact of variable accessible volume, we measured the ratio of fluorescence intensity in these regions to the intensity in immediately adjacent regions of rods expressing enhanced GFP or IFT52-GFP. The mean intensity ratio for GFP in the basal body region relative to the adjacent cytoplasm of the inner segment was 1.375 ± 0.145 (n=11), whereas that for IFT52-GFP was 10.42 ± 1.3 (n=41). The mean intensity ratio for GFP in the axonemal region relative to adjacent regions of the outer segment was 1.27 ± 0.056 (n=13), and the corresponding ratio for IFT52-GFP was 18.7 ± 10.14 (n=5). Thus, the degree of concentration of IFT52-GFP was 7.5 to 15 fold higher than for GFP alone in these regions.

In contrast to the targeted localization of IFT52-GFP and IFT57-GFP, less than 1% of embryos that were positive for IFT88-GFP transgenesis by genomic PCR showed any GFP signal by fluorescence microscopic analysis of the intact animal. Frozen sections of transgenic embryos in which no GFP fluorescence was detected by screening of the intact animal, revealed at most one or two cells expressing the GFP construct. In these cells, GFP fluorescence was sometimes concentrated in a discrete structure, possibly the basal body, at the apical end of the cell (Figure 5F). Light microscopy of one micron thick sections of plastic embedded IFT88-GFP embryos stained with toluidine blue often showed pyknotic nuclei in the photoreceptor layer and missing outer segments (Figure 6B, arrowheads); this was not observed in animals expressing GFP alone (Figure 6A). At the electron microscopic level, pyknotic nuclei (asterisk in Figure 6D) were often associated with fragments of both inner and outer segment that appeared to have been phagocytosed by the retinal pigmented epithelium (arrow in Figure 6D). In general, the rod inner and outer segments of IFT88-GFP animals were shorter and larger in diameter than those of animals expressing GFP, and sometimes had disorganized outer segments.

When IFT20-GFP was over-expressed in *Xenopus* rods, large aggregates of GFP accumulated in both the inner and the outer segments (not shown). There was no apparent localization of IFT20-GFP at the basal body or along the axonemes. Similar aggregates were observed in LLC-PK1 cells transiently transfected with CMV-IFT20-GFP (not shown). The finding that moderate to low expression of IFT20-GFP in stable kidney epithelial cell lines results in localization of the fusion protein to the Golgi complex and to cilia (Follit, Tuft, Fogarty & Pazour, 2006), suggests that that the aggregates formed in Xenopus rods and transiently transfected tissue culture cells are an artifact of strong over-expression of the fusion protein.

## DISCUSSION

### Importance of IFT in Photoreceptors

Our demonstration of the necessity of IFT88 in photoreceptors (Baker et al., 2003, Pazour et al., 2002) coupled with work on conditional deletion of the Kif3A subunit of kinesin II motor (Jimeno et al., 2006, Marszalek et al., 2000) have provided a strong case for the involvement of IFT in development and maintenance of photoreceptor outer segments. The requirement for both IFT88 and KIF3A is consistent with the role of kinesin 2 as an anterograde motor for IFT particles containing IFT88. This along with the demonstration of the photoreceptor expression of four IFT sub-particle B proteins (Pazour et al., 2002) and the finding that those same four IFT proteins can be isolated from photoreceptor cytosolic extracts as part of a larger ~17S IFT particle (Baker et al., 2003) similar to that from *Chlamydomonas* (Cole et al., 1998) indicate that the entire IFT sub-particle B is conserved in photoreceptors and functions in IFT transport in a manner similar to other cilium based systems. Although the earlier work demonstrated that IFT proteins were localized to the region of the connecting cilium (Pazour et al., 2002), the imaging was limited to frozen sections from bovine and mouse retina and did not resolve their distribution in the distal axoneme or in the periciliary cytoplasm. This raised the important question of whether IFT in photoreceptors was limited to the connecting cilium region between

the inner segment and newly assembled basal discs or, alternatively, extended distally into the outer segment.

## Localization of IFT Proteins in Photoreceptors

New data presented in this report add important details regarding the spatial distribution of IFT proteins in photoreceptors that are directly relevant to their function. First, IFT proteins are concentrated on and around the basal body and accessory centriole, consistent with the view that IFT particle assembly and docking occurs in this region of the cell (Deane et al., 2001). Immunogold images show that IFT88 is clustered in particulate structures. Although LR-White sections do not provide sufficient contrast for easy identification of membranes, many of the underlying immunogold labeled structures look like membrane vesicles. Since the individual 17S IFT sub-complex B is thought to have a single copy of IFT88 (Lucker, Behal, Qin, Siron, Taggart, Rosenbaum & Cole, 2005) and IFT88 immunoprecipitates principally with other IFT proteins (Baker et al., 2003), the clustering of IFT88 suggests that multiple copies of sub-complex B associate with each other and/or with other particulate structures. The peri-ciliary region of photoreceptors is known to be enriched in rhodopsin containing vesicles (Besharse & Pfenninger, 1980, Defoe & Besharse, 1985), which is mis-localized in Tg737$^{orpk}$ mice (Pazour et al., 2002). This raises the immediate possibility that IFT particles may associate with rhodopsin containing vesicles in the periciliary region. Multiple lines of evidence suggest that cilium membrane proteins require IFT for ciliary trafficking (Bae, Qin, Knobel, Hu, Rosenbaum & Barr, 2006, Follit et al., 2006, Qin, Burnette, Bae, Forscher, Barr & Rosenbaum, 2005) and recent analysis in cell culture suggest that membrane transport complexes assemble at the base of the cilium (Nachury, Loktev, Zhang, Westlake, Peranen, Merdes, Slusarski, Scheller, Bazan, Sheffield, Jackson, Miller, Summers, Hansen, Nachury, Lehman, Loktev & Jackson, 2007). These observations are consistent with work in progress indicating that both rhodopsin and photoreceptor membrane guanylyl cyclase 1 (GC1, Gucy2D) can be immunoprecipitated with IFT proteins (Bhowmick & Besharse, 2007).

Our new data also demonstrate that within the outer segment IFT proteins are localized in particulate structures along the entire length of the axoneme. Furthermore, in some cases the axoneme extends nearly the entire length (~50 μm in *Xenopus*) of the outer segment. This is expected based on the model from *Chlamydomonas* flagella in which a primary function of IFT is to support plus-end assembly/disassembly at the distal tip of the axoneme (Pedersen, Miller, Geimer, Leitch, Rosenbaum & Cole, 2005, Rosenbaum & Witman, 2002). In addition, several lines of evidence support the view that axonemal proteins are IFT cargo (Qin, Diener, Geimer, Cole & Rosenbaum, 2004). Since the axoneme of photoreceptor outer segments provides a structural backbone for elaboration of the photosensitive membrane discs, failure of proper outer segment formation in Tg737$^{orpk}$ mice could be an indirect consequence of impaired transport of axoneme components (Baker, Pazour, Witman & J.C., 2004, Besharse, Baker, Luby-Phelps & Pazour, 2003). In this regard both conservation of the components of IFT, and its cytoskeletal cargo would be expected in many types of motile and sensory cilia.

Consistent with the basal body and axoneme localization of endogenous IFT proteins, we have found that both IFT52-GFP and IFT57-GFP target to basal body and axoneme structures when over expressed at high levels in rod photoreceptors of transgenic *Xenopus*. This is consistent with work showing ciliary trafficking of YFP tagged Che-13 (Haycraft, Schafer, Zhang, Taulman & Yoder, 2003) and GFP tagged Osm-6 (Orozco, Wedaman, Signor, Brown, Rose & Scholey, 1999), the *C. elegans* homologues of IFT57 and IFT52 respectively. In contrast, IFT20-GFP was expressed at high levels but accumulated in large aggregates. One possible explanation is that the strong over-expression of IFT20-GFP driven by the opsin promoter may have caused artifactual intracellular aggregation of IFT20-GFP. In contrast to our results, stable

kidney epithelial cell lines expressing IFT20-GFP at low levels, the fusion protein targets to the Golgi-complex and cilium in a manner similar to endogenous IFT20 (Follit et al., 2006).

The low expression of IFT88-GFP in *Xenopus* photoreceptors was surprising, especially given the robust expression of the other three constructs, which differ only in the primary sequence of the insert. The same IFT88-GFP insert was expressed at high levels when transfected into tissue culture cells using a CMV-driven vector (data not shown). Possible reasons for the low expression of the IFT88-GFP cDNA in the rods of transgenic animals include the absence of important untranslated regions of the gene, rapid degradation of the expressed protein, or death of cells that express the protein at a high level. Light and electron microscopic analysis of sectioned eyes from animals that were positive for transgenesis by genomic PCR, but negative for expression of IFT88-GFP, showed pyknotic nuclei and abnormalities in the morphology of the rods, consistent with the latter possibility. This could result from impaired functionality of IFT88 due to the presence of the GFP tag, or simply the over-expression of the functional protein. In this regard, it has already been shown that mouse photoreceptors are particularly sensitive to IFT88 concentration because the 5−10 fold reduction in IFT88 levels in $Tg737^{orpk}$ mice results in photoreceptor degeneration (Pazour et al., 2002).

## Photoreceptors as a Model System for IFT

The importance of IFT in ciliated cells is underscored by the large number of recent studies showing that IFT is required for both development and function of cilia in multiple cell types. Many conserved features of IFT such as IFT sub-complexes A and B and the dynein and kinesin 2 motor are likely to be common to multiple cell types and rapid progress on these features of IFT is likely to take place in simple model organisms. Nonetheless, photoreceptors represent an ideal model system for analysis of key features such as IFT cargo, IFT motors, and IFT signaling. For example, a critical question related to photoreceptor specific IFT is whether it is simply required to build the axonemal backbone of the outer segment as in other cilium types, or whether outer segment specific phototransduction proteins are transported by IFT. Both rhodopsin and arrestin are miss-localized in photoreceptors deficient in Kif3A and rhodopsin is mislocalized in $Tg737^{orpk}$ mice (Pazour et al., 2002), which has led to the suggestion that both are transported by kinesin 2 (Marszalek et al., 2000). Nonetheless, miss-localization of rhodopsin occurs secondary to a variety stressful insults to photoreceptors. Furthermore, available data on the kinetics, magnitude, and ATP dependence of arrestin movement in light suggest that diffusion coupled with light regulation of binding sites could account for its movement to the outer segment (Calvert, Strissel, Schiesser, Pugh & Arshavsky, 2006, Nair, Hanson, Mendez, Gurevich, Kennedy, Shestopalov, Vishnivetskiy, Chen, Hurley, Gurevich & Slepak, 2005). On the other hand, substantial evidence has emerged linking cilium membrane protein trafficking to IFT, including recent data showing IFT dependent translocation of TRPV channels within the cilium (Qin et al., 2005). In photoreceptors we think that the strongest current case for outer segment specific IFT cargo is for membrane guanylyl cyclase 1 (GC1) and rhodopsin, which co-immuprecipitate with IFT proteins and the kinesin II motor (Bhowmick & Besharse, 2007). Furthermore, deletion of both GC1 and GC2 causes miss-localization of additional membrane associated outer segment proteins, which has led to the suggestion that those proteins may normally be co-transported with membrane guanylyl cyclase (Baehr, Karan, Maeda, Luo, Li, Bronson, Watt, Yau, Frederick & Palczewski, 2007).

Classically, kinesin II and cytoplasmic dynein heavy chain 1b (Dhc1b) have been described as the anterograde and retrograde IFT motors. However, emerging data in *C. elegans* suggest that both kinesin II and an accessory IFT kinesin called Osm-3 serve as IFT kinesins with different roles depending on the sensory cilium type (Evans, Snow, Gunnarson, Ou, Stahlberg, McDonald & Scholey, 2006, Snow et al., 2004). In particular, it has been proposed that Osm-3, a homodimeric kinesin, is required in amphid channel cilia whose doublet microtubules give

way to singlet microtubules in the distal segment. Although a comparable role for the Osm-3 homologue, Kif17, in vertebrates has not been identified, distal segments of photoreceptor outer segments are known to contain singlet microtubules (Roof, Adamian, Jacobs & Hayes, 1991, Steinberg & Wood, 1975). Recently, we found that Kif17 is co-localized with IFT proteins in zebrafish photoreceptors and that antisense knockdown of Kif17 in embryos caused a failure of outer segment formation. Under the same conditions, cilium elongation in kidney epithelial cells occurs normally (Insinna & Besharse, 2007). These results suggest that Kif17 is not essential for kidney cilium elongation, but is essential in photoreceptors.

Since many cilia including photoreceptor outer segments are sensory organelles, the requirement for IFT in cilium assembly places it upstream of a wide array of biologically significant signaling pathways including phototransduction (Pan, Wang & Snell, 2005). Perhaps more important for photoreceptor biology, however, is the question of whether reciprocal IFT between the outer and inner segment could play a direct and more immediate signaling role. For example, in rod cells both transducin subunits (Gtα and Gtβ) and arrestin are known to translocate in opposite directions between the segments in the light and dark, and physiological analysis has shown that movement to the inner segment reduces visual sensitivity in bright light (Calvert et al., 2006, Sokolov et al., 2002). Clearly, this means that the translocation event itself is one component of sensory adaptation. The question that arises is whether IFT plays a role in Gtα and Gtβ or arrestin translocation. An answer to this question is not yet available and would require an understanding of how those proteins regulate their association with the IFT machinery. Nonetheless, the current debate pits molecular motors against simple diffusion. In the case of light driven translocation of arrestin and Gtα, data on the kinetics and magnitude of the event favor a diffusional mechanism (Calvert et al., 2006). The reversal of those movements during dark adaptation, however, occurs more slowly and is compatible with molecular motor driven pathways.

**ACKNOWLEDGEMENTS**

We are very grateful to Dr. Gregory Ning from the Medical College of Wisconsin EM Facility for assistance with the electron microscopy. Some of the data in this report were presented at the 2002 annual meeting of the American Society for Cell Biology of Cell Biology and the 2003 annual meeting of the Association for Research in Vision and Ophthalmology. This research was supported by grants from the National Science Foundation (NSF MCB 9604594, KLP) and the National Institutes of Health (NIH EY03222, JCB).

## References

Bae YK, Qin H, Knobel KM, Hu J, Rosenbaum JL, Barr MM. General and cell-type specific mechanisms target TRPP2/PKD-2 to cilia. Development 2006;133(19):3859–3870. [PubMed: 16943275]

Baehr W, Karan S, Maeda T, Luo DG, Li S, Bronson JD, Watt CB, Yau KW, Frederick JM, Palczewski K. The function of guanylate cyclase 1 and guanylate cyclase 2 in rod and cone photoreceptors. J Biol Chem 2007;282(12):8837–8847. [PubMed: 17255100]Epub 2007 Jan 8825

Baker SA, Freeman K, Luby-Phelps K, Pazour GJ, Besharse JC. IFT20 links kinesin II with a mammalian intraflagellar transport complex that is conserved in motile flagella and sensory cilia. J Biol Chem 2003;278(36):34211–34218. [PubMed: 12821668]

Baker, SA.; Pazour, GJ.; Witman, GB.; J.C., J. Photoreceptors and Intraflagellar Transport.. In: Williams, DA., editor. Photoreceptor Cell Biology and Inherited Retinal Degenerations. 10. WORLD SCIENTIFIC PUBLISHING COMPANY PTE LTD; Singapore: 2004. p. 109-132.

Beech PL, Pagh-Roehl K, Noda Y, Hirokawa N, Burnside B, Rosenbaum JL. Localization of kinesin superfamily proteins to the connecting cilium of fish photoreceptors. Journal of Cell Science 1996;109:889–897. [PubMed: 8718680]

Besharse JC, Baker SA, Luby-Phelps K, Pazour GJ. Photoreceptor intersegmental transport and retinal degeneration: a conserved pathway common to motile and sensory cilia. Adv Exp Med Biol 2003;533:157–164. [PubMed: 15180260]

Besharse, JC.; Horst, CJ. The photoreceptor connecting cilium. A model for the transition zone.. In: Bloodgood, RA., editor. Ciliary and Flagellar Membranes. Plenum Publishing Corp; New York: 1990. p. 389-417.

Besharse JC, Pfenninger KH. Membrane assembly in retinal photoreceptors I. freeze-fracture analysis of cytoplasmic vesicles in relationship to disc assembly. Journal of Cell Biology 1980;87:451–463. [PubMed: 7430251]

Bhowmick, R.; Besharse, JC. Identification of a Chaperone Mediated Cargo Complex Association With Intraflagellar Transport Proteins in Photoreceptor.. Annual Meeting of Association of Research in Vision and Ophthalmology. 2007. Abstract 3799.Full length abstracts at: http://www.arvo.org

Cahill GM, Besharse JC. Resetting the circadian clock in cultured *Xenopus* eyecups: regulation of retinal melatonin rhythms by light and D2 dopamine receptors. Journal of Neuroscience 1991;11:2959–2971. [PubMed: 1682423]

Calvert PD, Strissel KJ, Schiesser WE, Pugh EN Jr. Arshavsky VY. Light-driven translocation of signaling proteins in vertebrate photoreceptors. Trends Cell Biol 2006;16(11):560–568. [PubMed: 16996267]

Cole DG, Diener DR, Himelblau AL, Beech PL, Fuster JC, Rosenbaum JL. Chlamydomonas kinesin-II-dependent intraflagellar transport (IFT): IFT particles contain proteins required for ciliary assembly in *Caenorhabditis elegans* sensory neurons. Journal of Cell Biology 1998;141:993–1008. [PubMed: 9585417]

Deane JA, Cole DG, Seeley ES, Diener DR, Rosenbaum JL. Localization of intraflagellar transport protein IFT52 identifies basal body transitional fibers as the docking site for IFT particles. Curr Biol 2001;11(20):1586–1590. [PubMed: 11676918]

Defoe DM, Besharse JC. Membrane assembly in retinal photoreceptors II. immunocytochemical analysis of freeze-fractured rod photoreceptor membranes using anti-opsin antibodies. Journal of Neuroscience 1985;5(4):1023–1034. [PubMed: 3156972]

Evans JE, Snow JJ, Gunnarson AL, Ou G, Stahlberg H, McDonald KL, Scholey JM. Functional modulation of IFT kinesins extends the sensory repertoire of ciliated neurons in Caenorhabditis elegans. J Cell Biol 2006;172(5):663–669. [PubMed: 16492809]

Follit JA, Tuft RA, Fogarty KE, Pazour GJ. The intraflagellar transport protein IFT20 is associated with the Golgi complex and is required for cilia assembly. Mol Biol Cell 2006;17(9):3781–3792. [PubMed: 16775004]

Haycraft CJ, Schafer JC, Zhang QH, Taulman PD, Yoder BK. Identification of CHE-13, a novel intraflagellar transport protein required for cilia formation. Exp Cell Res 2003;284(2):251–263. [PubMed: 12651157]

Insinna, C.; Besharse, JC. The Homodimeric Kinesin, KIF17, Is Required for Photoreceptor Outer Segment Development.. Annual Meeting of Association of Research in Vision and Ophthalmology. 2007. Abstract 4658.Full length abstracts at: http://www.arvo.org

Jimeno D, Feiner L, Lillo C, Teofilo K, Goldstein LS, Pierce EA, Williams DS. Analysis of kinesin-2 function in photoreceptor cells using synchronous Cre-loxP knockout of Kif3a with RHO-Cre. Invest Ophthalmol Vis Sci 2006;47(11):5039–5046. [PubMed: 17065525]

Kaplan MW, Iwata RT, Sears RC. Lengths of immunolabeled ciliary microtubules in frog photoreceptor outer segments. Experimental Eye Research 1987;44:623–632. [PubMed: 2887449]

Kennedy BN, Vihtelic TS, Checkley L, Vaughan KT, Hyde DR. Isolation of a zebrafish rod opsin promoter to generate a transgenic zebrafish line expressing enhanced green fluorescent protein in rod photoreceptors. J Biol Chem 2001;276(17):14037–14043. [PubMed: 11278688]

Knox BE, Schlueter C, Sanger BM, Green CB, Besharse JC. Transgene expression in *Xenopus* rods. Federation of European Biochemical Societies 1998;423:117–121.

Kozminski KG, Beech PL, Rosenbaum JL. The *Chlamydomonas* kinesin-like protein FLA10 is involved in motility associated with the flagellar membrane. Journal of Cell Biology 1995;131:1517–1527. [PubMed: 8522608]

Kozminski KG, Johnson KA, Forscher P, Rosenbaum JL. A motility in the eukaryotic flagellum unrelated to flagellar beating. Proceedings of the National Academy of Sciences of the United States of America 1993;90:5519–5523. [PubMed: 8516294]

Lucker BF, Behal RH, Qin H, Siron LC, Taggart WD, Rosenbaum JL, Cole DG. Characterization of the intraflagellar transport complex B core: direct interaction of the IFT81 and IFT74/72 subunits. J Biol Chem 2005;280(30):27688–27696. [PubMed: 15955805]

Marszalek JR, Liu X, Roberts EA, Chui D, Marth JD, Williams DS, Goldstein LS. Genetic evidence for selective transport of opsin and arrestin by kinesin-II in mammalian photoreceptors. Cell 2000;102 (2):175–187. [PubMed: 10943838]

Mendez A, Lem J, Simon M, Chen J. Light-dependent translocation of arrestin in the absence of rhodopsin phosphorylation and transducin signaling. J Neurosci 2003;23(8):3124–3129. [PubMed: 12716919]

Nachury MV, Loktev AV, Zhang Q, Westlake CJ, Peranen J, Merdes A, Slusarski DC, Scheller RH, Bazan JF, Sheffield VC, Jackson PK, Miller JJ, Summers MK, Hansen DV, Nachury MV, Lehman NL, Loktev A, Jackson PK. A Core Complex of BBS Proteins Cooperates with the GTPase Rab8 to Promote Ciliary Membrane Biogenesis. Cell 2007;129(6):1201–1213. [PubMed: 17574030]

Nair KS, Hanson SM, Mendez A, Gurevich EV, Kennedy MJ, Shestopalov VI, Vishnivetskiy SA, Chen J, Hurley JB, Gurevich VV, Slepak VZ. Light-dependent redistribution of arrestin in vertebrate rods is an energy-independent process governed by protein-protein interactions. Neuron 2005;46(4):555–567. [PubMed: 15944125]

Orozco JT, Wedaman KP, Signor D, Brown H, Rose L, Scholey JM. Movement of motor and cargo along cilia. Nature 1999;398:674. [PubMed: 10227290]

Pan J, Wang Q, Snell WJ. Cilium-generated signaling and cilia-related disorders. Lab Invest 2005;85(4): 452–463. [PubMed: 15723088]

Pazour GJ, Baker SA, Deane JA, Cole DG, Dickert BL, Rosenbaum JL, Witman GB, Besharse JC. The intraflagellar transport protein, IFT88, is essential for vertebrate photoreceptor assembly and maintenance. J Cell Biol 2002;157(1):103–113. [PubMed: 11916979]

Pazour GJ, Dickert BL, Witman GB. The DHC1b (DHC2) isoform of cytoplasmic dynein is required for flagellar assembly. Journal of Cell Biology 1999;144:473–481. [PubMed: 9971742]

Pazour GJ, Wilkerson CG, Witman GB. A dynein light chain is essential for the retrograde particle movement of intraflagellar transport (IFT). Journal of Cell Biology 1998;141:979–992. [PubMed: 9585416]

Pedersen LB, Miller MS, Geimer S, Leitch JM, Rosenbaum JL, Cole DG. Chlamydomonas IFT172 is encoded by FLA11, interacts with CrEB1, and regulates IFT at the flagellar tip. Curr Biol 2005;15 (3):262–266. [PubMed: 15694311]

Peet JA, Bragin A, Calvert PD, Nikonov SS, Mani S, Zhao X, Besharse JC, Pierce EA, Knox BE, Pugh EN Jr. Quantification of the cytoplasmic spaces of living cells with EGFP reveals arrestin-EGFP to be in disequilibrium in dark adapted rod photoreceptors. J Cell Sci 2004;117(Pt 14):3049–3059. [PubMed: 15197244]

Peterson JJ, Tam BM, Moritz OL, Shelamer CL, Dugger DR, McDowell JH, Hargrave PA, Papermaster DS, Smith WC. Arrestin migrates in photoreceptors in response to light: a study of arrestin localization using an arrestin-GFP fusion protein in transgenic frogs. Exp Eye Res 2003;76(5):553–563. [PubMed: 12697419]

Qin H, Burnette DT, Bae YK, Forscher P, Barr MM, Rosenbaum JL. Intraflagellar transport is required for the vectorial movement of TRPV channels in the ciliary membrane. Curr Biol 2005;15(18):1695–1699. [PubMed: 16169494]

Qin H, Diener DR, Geimer S, Cole DG, Rosenbaum JL. Intraflagellar transport (IFT) cargo: IFT transports flagellar precursors to the tip and turnover products to the cell body. J Cell Biol 2004;164(2):255–266. [PubMed: 14718520]

Roof D, Adamian M, Jacobs D, Hayes A. Cytoskeletal specializations at the rod photoreceptor distal tip. Journal of Comparative Neurology 1991;305:289–303. [PubMed: 1902849]

Rosenbaum JL, Witman GB. Intraflagellar transport. Nat Rev Mol Cell Biol 2002;3(11):813–825. [PubMed: 12415299]

Sale WS, Besharse JC, Piperno G. Distribution of acetylated α-tubulin in retina and in in vitro-assembled microtubules. Cell Motility and the Cytoskeleton 1988;9:243–253. [PubMed: 3259167]

Scholey JM. Intraflagellar transport. Annu Rev Cell Dev Biol 2003;19:423–443. [PubMed: 14570576]

Signor D, Wedaman KP, Orozco JT, Dwyer ND, Bargmann CI, Rose LS, Scholey JM. Role of a class DHC1b dynein in retrograde transport of IFT motors and IFT raft particles along cilia, but not

dendrites, in chemosensory neurons of living *Caenorhabditis elegans*. Journal of Cell Biology 1999;147:519–530. [PubMed: 10545497]

Sloboda RD. Intraflagellar transport and the flagellar tip complex. J Cell Biochem 2005;94(2):266–272. [PubMed: 15558569]

Snow JJ, Ou G, Gunnarson AL, Walker MR, Zhou HM, Brust-Mascher I, Scholey JM. Two anterograde intraflagellar transport motors cooperate to build sensory cilia on C. elegans neurons. Nat Cell Biol 2004;6(11):1109–1113. [PubMed: 15489852]

Sokolov M, Lyubarsky AL, Strissel KJ, Savchenko AB, Govardovskii VI, Pugh EN Jr. Arshavsky VY. Massive light-driven translocation of transducin between the two major compartments of rod cells: a novel mechanism of light adaptation. Neuron 2002;34(1):95–106. [PubMed: 11931744]

Steinberg RH, Wood I. Clefts and microtubules of photoreceptor outer segments in the retina of the domestic cat. J Ultrastruct Res 1975;51(3):307–403. [PubMed: 1138108]

Swaminathan R, Hoang CP, Verkman AS. Photobleaching recovery and anisotropy decay of green fluorescent protein GFP-S65T in solution and cells: cytoplasmic viscosity probed by green fluorescent protein translational and rotational diffusion. Biophys J 1997;72(4):1900–1907. [PubMed: 9083693]

Taylor DL, Wang YL. Fluorescently labelled molecules as probes of the structure and function of living cells. Nature 1980;284(5755):405–410. [PubMed: 6987537]

Terry BR, Matthews EK, Haseloff J. Molecular characterisation of recombinant green fluorescent protein by fluorescence correlation microscopy. Biochem Biophys Res Commun 1995;217(1):21–27. [PubMed: 8526912]

Tsujikawa M, Malicki J. Intraflagellar transport genes are essential for differentiation and survival of vertebrate sensory neurons. Neuron 2004;42(5):703–716. [PubMed: 15182712]

Yokoe H, Meyer T. Spatial dynamics of GFP-tagged proteins investigated by local fluorescence enhancement. Nat Biotechnol 1996;14(10):1252–1256. [PubMed: 9631088]

Young RW. The renewal of photoreceptor cell outer segments. Journal of Cell Biology 1967;33:61–72. [PubMed: 6033942]

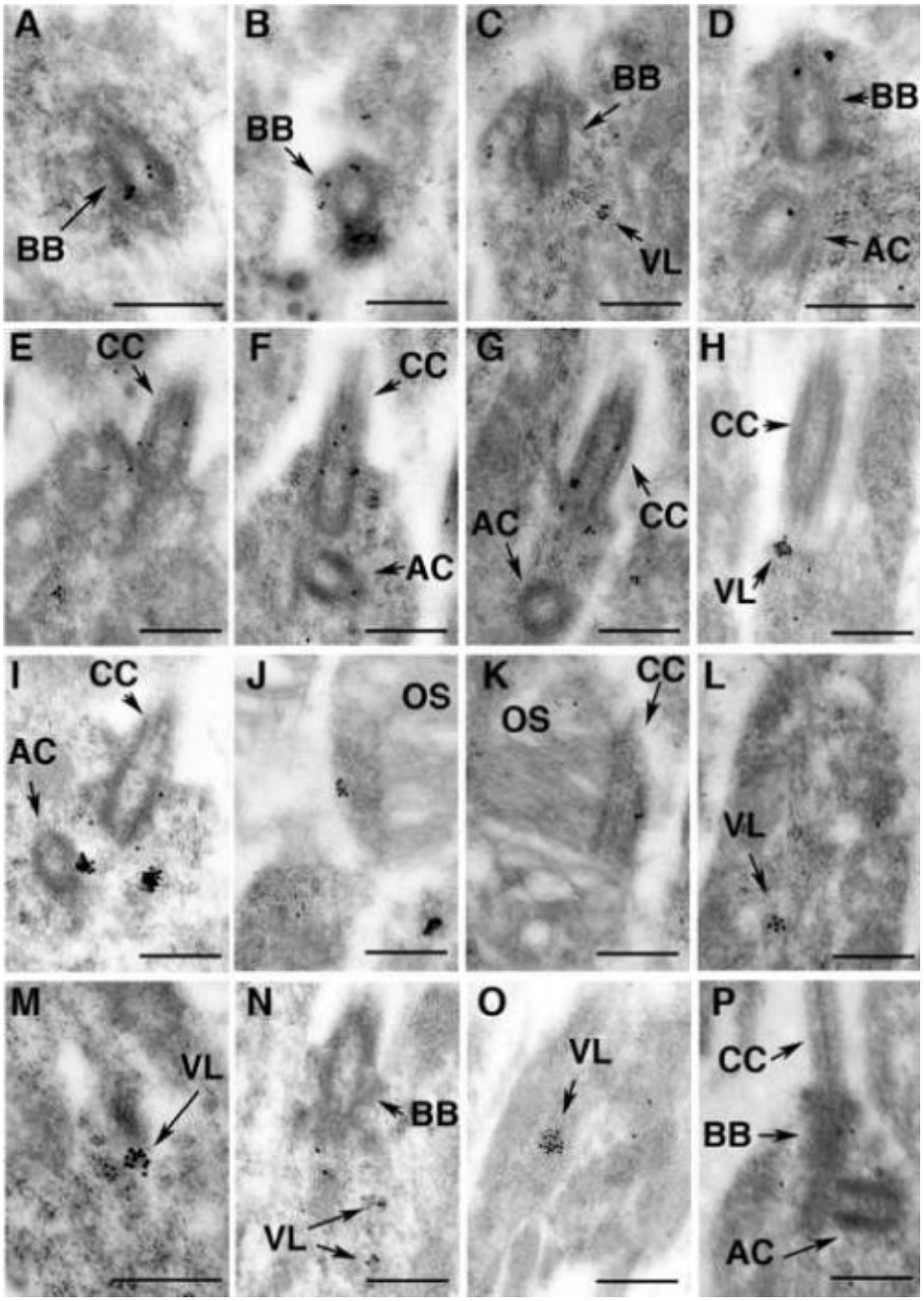


**Figure 1.**

Immunogold localization of IFT88 in mouse rods using 10 nanometer colloidal gold. A-P is a panel of images taken in the vicinity of the basal body (BB) and connecting cilium (CC); A-O are from wildtype mice and P is from a $Tg737^{orpk}$ retina prepared at 21 postnatal days. Note that $Tg737^{orpk}$ mice carry a hypomorphic mutation in IFT88 and express WT protein at 5−10 fold lower levels than WT. Positive staining for IFT88 was seen at the basal body (BB), accessory centriole (AC), the connecting cilium (CC), the axoneme region adjacent to discs (OS, see J and K), and in particulate, vesicle-like (VL) structures in the inner segment. Bars in the lower right of each image are 1 μm in length.

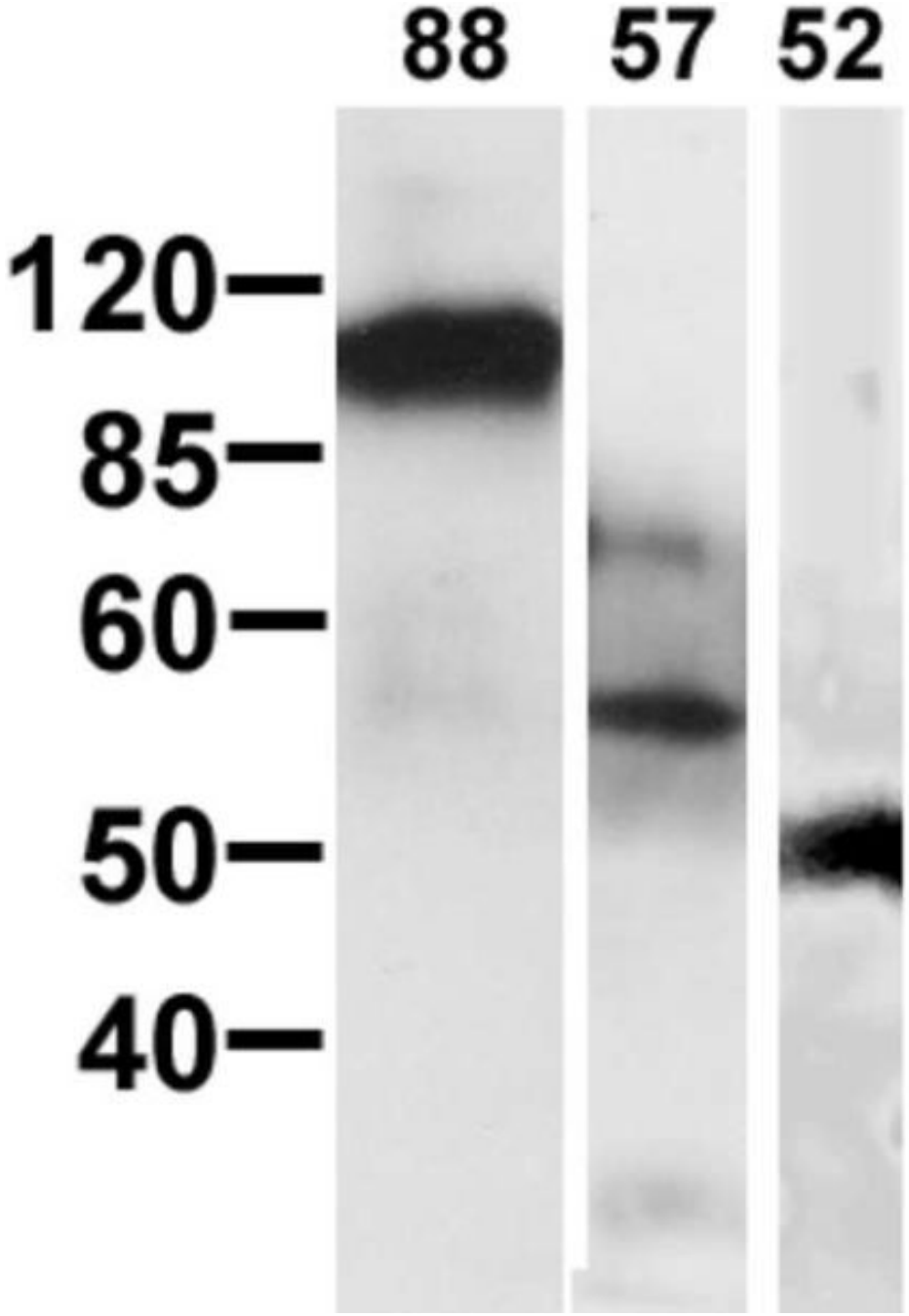


**Figure 2.**
Western blot of IFT proteins in adult *Xenopus* retina. Retina extracts from adult *Xenopus laevis* were probed with rabbit antibodies to mouse IFT88, 57, 52 and 20. Bands of the approximate molecular weight for IFT88, 57 and 52 were detected as indicated. Bands were not detected by the antibody against IFT20.

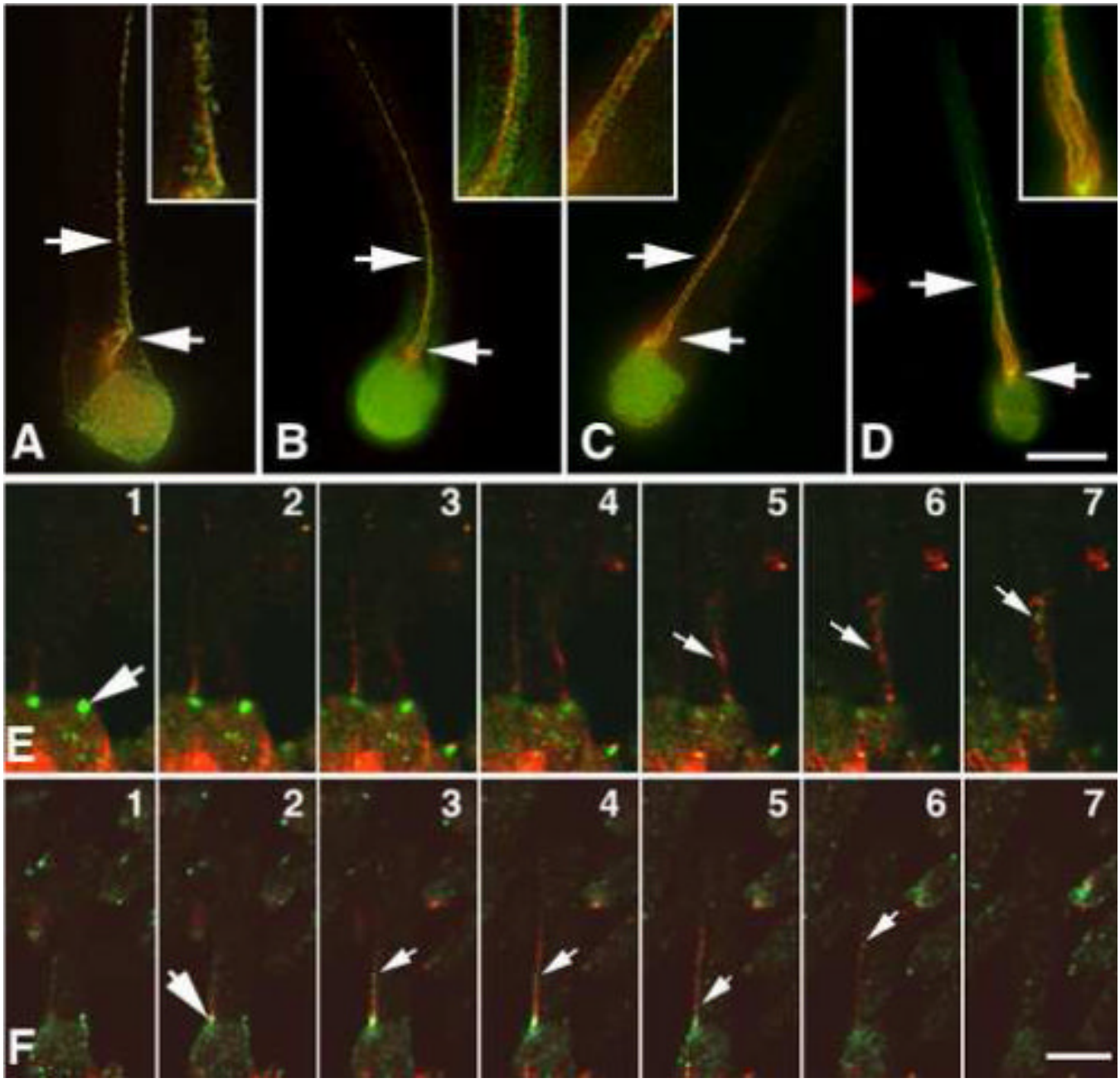


**Figure 3.**

Immunofluorescence localization of IFT proteins in *Xenopus leavis* photoreceptors. A-D. Dissociated rod outer segments with attached inner segments were double labeled with antibodies to acetylated-alpha-tubulin (red) and IFT proteins (green); IFT88 (A), IFT57 (B) IFT52 (C), andIFT20 (D). Axonemes are rooted in the brightly fluorescent ellipsoids of the inner segment below and extend distally into the outer segment. IFT proteins are localized within the ellipsoid region and along the axoneme (arrows), often in discrete particles. The insets are 2× enlargements of the axoneme segment between the two arrows, which more clearly reveal of particulate nature of IFT staining. E. Confocal Z-series (1−7) of a frozen section double labeled with antibodies to acetylated alpha-tubulin (red) and IFT57 (green) showing the extensive accumulation of IFT protein at the base of the axoneme in the vicinity

of the basal body (large arrow) and particulate staining along the axoneme (small arrows). F. Confocal Z-series similar to E but labeled with an antibody to IFT20 (green); large arrow indicates the base of the axoneme and small arrows indicate particles on axoneme.

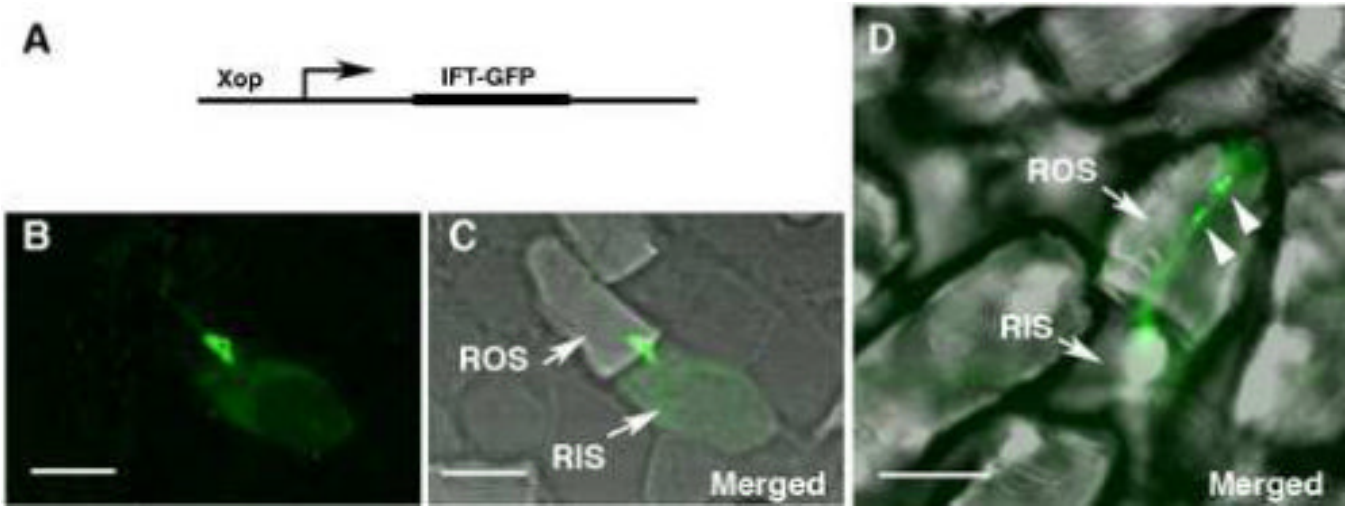


**Figure 4.**

Expression of IFT52-GFP in *Xenopus* rods. Isolated retinas from transgenic animals were viewed by confocal microscopy. A. Diagram illustrating the general design of the IFT-GFP constructs driven by the *Xenopus* opsin promotor as described previously (Knox et al., 1998). B. GFP image of a rod. C. Same GFP image as in B merged with a transmitted light image showing the position of the rod inner (RIS) and outer segments (ROS). C. Similar merged imaged showing IFT52-GFP extending along the axoneme (arrow) with occasional particles (small arrows). Scale bars: 5 μm.

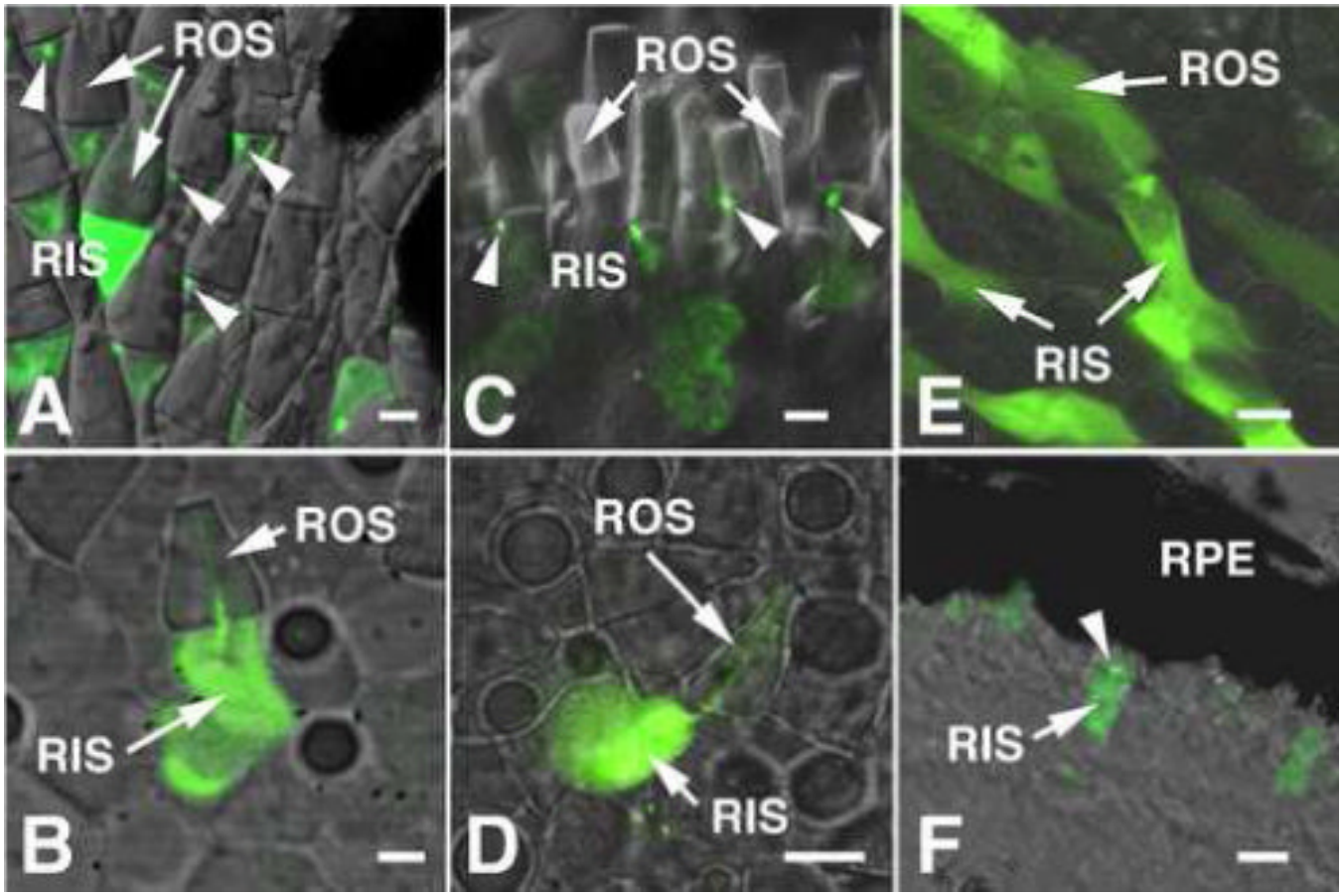


**Figure 5.**

Localization of over-expressed IFT-GFP constructs in transgenic *Xenopus* rods. The green GFP fluorescence image is superimposed on the transmitted light image as in Figure 4. A-B. A low and higher power image of IFT52-GFP. C-D. A low and higher power image of IFT57-GFP. E: Image showing free GFP. F. Frozen section from an eye expressing IFT88-GFP showing localization of fluorescence at the basal body (arrowhead). Note that for both IFT52 and IFT57 fluorescence appeared concentrated at the basal body (A and C, arrowheads) and extended into the ROS along an axoneme-like structure (B & D). Fluorescence in rods expressing GFP alone was diffuse throughout the cell and spatial variations in intensity were due to differences in accessible volume (E). Abbreviations: ROS, rod outer segment; RIS, rod inner segment; RPE, retina pigment epithelium. Scale bars: 5 μm A-E; 20 μm F.

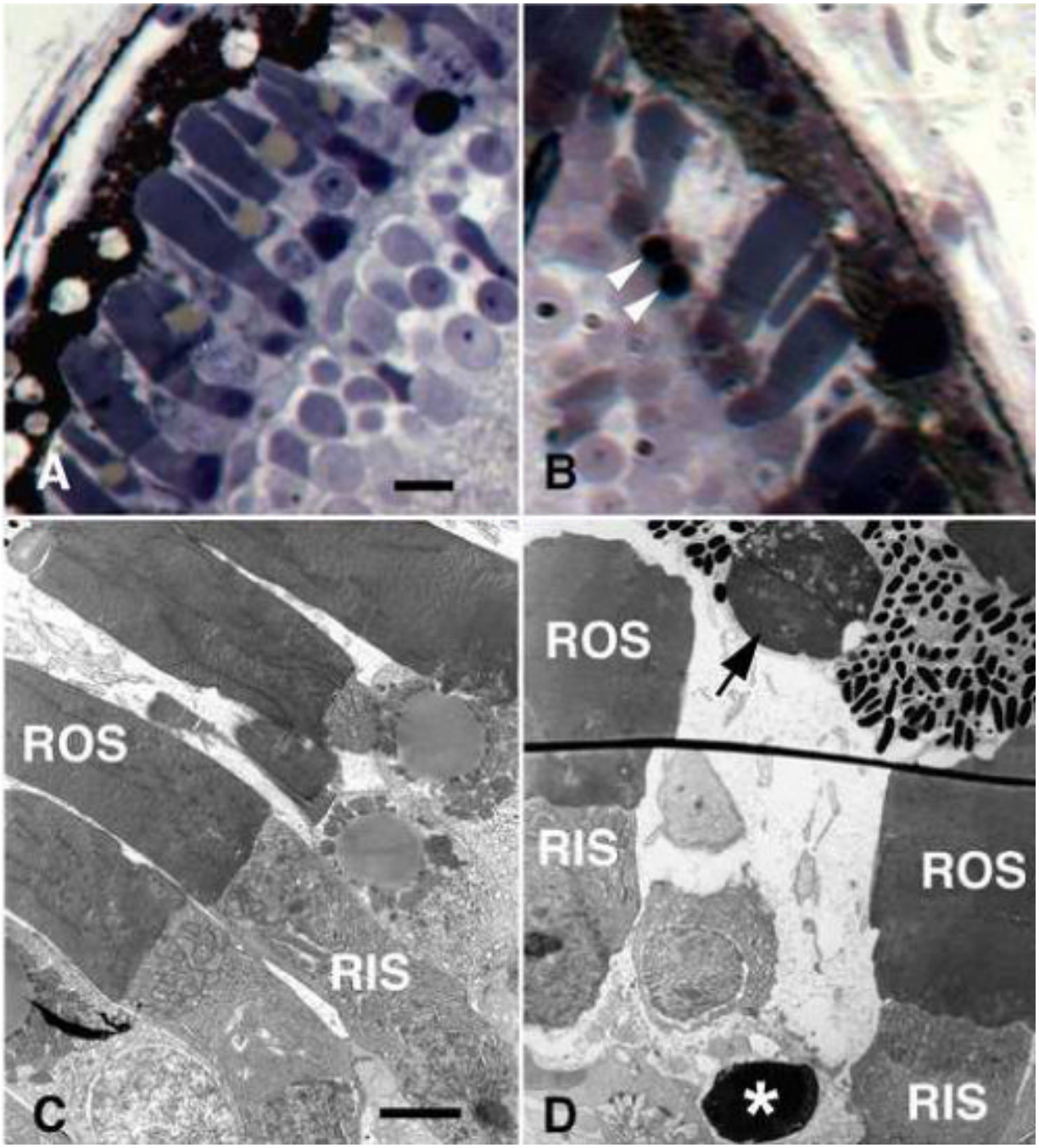


**Figure 6.**

Light and electron microscopic morphology of retinas of *Xenopus* tadpoles whose rods were expressing either GFP alone or IFT88-GFP. A & C: Retinas from stage 45 control animals transgenic for GFP alone. B & D: Retinas from stage 45 animals transgenic for IFT88-GFP. At the light microscopic level, pyknotic nuclei (B, arrowheads) and missing outer segments were observed in retinas expressing IFT88-GFP. By electron microscopy, fragments of inner segment were frequently observed embedded in the retinal pigmented epithelium (D, arrowhead) in association with pyknotic nuclei (D, asterisk). In general, the rods in retinas expressing IFT88-GFP were shorter and broader than in control retinas. Abbreviations: RPE,

retinal pigmented epithelium; ROS, rod outer segment; RIS, rod inner segment. Scale bars: 10 μm A and B; 5 μm C and D.